

CLASSIFICATION OF 2-COMPONENT VIRTUAL LINKS UP TO Ξ -MOVES

JEAN-BAPTISTE MEILHAN, SHIN SATOH, AND KODAI WADA

ABSTRACT. The Ξ -move is a local move generated by forbidden moves in virtual knot theory. This move was introduced by Taniguchi and the second author, who showed that it characterizes the odd writhe of virtual knots, which is a fundamental invariant defined by Kauffman. In this paper, we extend this result by classifying 2-component virtual links up to Ξ -moves, using refinements of the odd writhe and linking numbers.

1. INTRODUCTION

Virtual knot theory developed by Kauffman in [5] is a diagrammatic extension of the classical study of knots in 3-space. A *virtual knot* is a generalized knot diagram, where one allows both classical and virtual crossings, regarded up to an extended set of Reidemeister moves. Alternatively, virtual knots can be described in terms of *Gauss diagrams*, which are copies of S^1 endowed with signed and oriented chords, modulo certain deformations [3]. The set-theoretic inclusion of usual knot diagrams into virtual knot diagrams induces an injection of classical knots into virtual knots.

In virtual knot theory, we cannot pass a strand ‘over’ or ‘under’ a virtual crossing. These operations are called the *forbidden moves*. At the Gauss diagram level, forbidden moves allow to exchange the relative positions of any two consecutive endpoints P_1 and P_2 of chords on a circle. See the left of Figure 1.1, where ε_i are the signs of chords. It is known that any virtual knot is deformed into the trivial knot by forbidden moves [4, 10]. Generally, the μ -component virtual links $L = K_1 \cup \dots \cup K_\mu$ up to forbidden moves are classified by the (i, j) -linking numbers $\text{Lk}(K_i, K_j)$ ($1 \leq i \neq j \leq \mu$) completely [1, 9, 12].

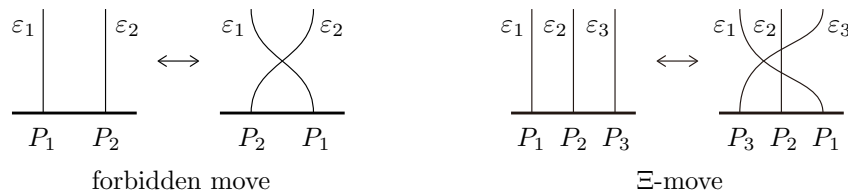


FIGURE 1.1. The forbidden moves and Ξ -moves on Gauss diagrams

The purpose of this paper is to study an operation called the Ξ -move, which is generated by forbidden moves. At the Gauss diagram level, a Ξ -move swaps the positions of P_1 and P_3 of three consecutive endpoints $P_1, P_2,$ and P_3 of chords. See the right of Figure 1.1. The Ξ -move arises naturally as a characterization of virtual knots having the same odd writhe. Here the *odd writhe* $J(K)$ is a fundamental invariant of a virtual knot K in virtual knot theory defined by Kauffman in [6]. In [13], Taniguchi and the second author proved the following.

2020 *Mathematics Subject Classification*. Primary 57K12; Secondary 57K10.

Key words and phrases. virtual link, Ξ -move, odd writhe, linking class, Gauss diagram.

Theorem 1.1 ([13, Theorem 1.7]). *Let K and K' be virtual knots. Then the following are equivalent.*

- (i) K and K' are related by a finite sequence of Ξ -moves.
- (ii) $J(K) = J(K')$.

We remark that Ohyama and Yoshikawa [11] obtained the same result independently.

In this paper, we push further this study by classifying 2-component virtual links up to Ξ -moves. The situation turns out to be very different depending on the *parity* of a virtual link. A 2-component virtual link is called *odd* (resp. *even*) if the number of classical crossings involving both components is odd (resp. even) (Definition 2.3). Notice that the set of 2-component even virtual links contains that of classical 2-component links.

In the odd case, we have the following.

Theorem 1.2. *Let $L = K_1 \cup K_2$ and $L' = K'_1 \cup K'_2$ be 2-component odd virtual links. Then the following are equivalent.*

- (i) L and L' are related by a finite sequence of Ξ -moves.
- (ii) $\text{Lk}(K_1, K_2) = \text{Lk}(K'_1, K'_2)$ and $\text{Lk}(K_2, K_1) = \text{Lk}(K'_2, K'_1)$.

We remark that each component of a 2-component odd virtual link can be unknotted by Ξ -moves. Furthermore, by the classification of 2-component virtual links up to forbidden moves [12, Corollary 7] (see also [1, Proposition 3.6]), Theorem 1.2 means that the equivalence relation generated by Ξ -moves is coincident with that by forbidden moves on the set of 2-component odd virtual links.

The even case is much less simple, and involves three new invariants. For a 2-component even virtual link $L = K_1 \cup K_2$, we introduce the odd writhe of the pair (L, K_i) for $i = 1, 2$, denoted by $J(L, K_i)$, as an extension of the original invariant defined in [6] (Definition 6.3). Furthermore, we define the reduced linking class $\overline{F}(L)$ of L , which is a refinement of the linking numbers $\text{Lk}(K_1, K_2)$ and $\text{Lk}(K_2, K_1)$ (Definition 6.6). Then we have the following.

Theorem 1.3. *Let $L = K_1 \cup K_2$ and $L' = K'_1 \cup K'_2$ be 2-component even virtual links. Then the following are equivalent.*

- (i) L and L' are related by a finite sequence of Ξ -moves.
- (ii) $J(L, K_1) = J(L', K'_1)$, $J(L, K_2) = J(L', K'_2)$, and $\overline{F}(L) = \overline{F}(L')$.

This paper is organized as follows. In Section 2, we review the definitions of virtual links and Gauss diagrams. The proof of Theorem 1.2 is given in Section 3 by showing that a forbidden move is generated by Ξ -moves in the case of 2-component odd virtual links. In Section 4, we study shells, which are a certain kind of self-chords in a Gauss diagram, and prove that any Gauss diagram can be deformed into a certain form with shells up to Ξ -moves (Proposition 4.5). In Section 5, we introduce the notion of a ladder consisting of parallel nonself-chords in a Gauss diagram, and give a representative of the equivalence class of a 2-component virtual link under Ξ -moves (Proposition 5.12). In Section 6, we define three kinds of invariants $J(L, K_1)$, $J(L, K_2)$, and $\overline{F}(L)$ of a 2-component even virtual link $L = K_1 \cup K_2$, and establish a relationship among these invariants (Theorem 6.10). The last section is devoted to the proof of Theorem 1.3.

Acknowledgements. The authors would like to thank Professors Takuji Nakamura and Yasutaka Nakanishi for useful comments and suggestions on an early version of the paper. They also thank the referee for the careful reading of the paper and for his/her comments and suggestions. The first author was partly supported by the project AIMaRe (ANR-19-CE40-0001-01) of the ANR. The second author was

partially supported by JSPS KAKENHI Grant Number JP19K03466. The third author was partially supported by JSPS KAKENHI Grant Number JP19J00006.

2. VIRTUAL LINKS AND GAUSS DIAGRAMS

For an integer $\mu \geq 1$, a μ -component virtual link diagram is the image of an immersion of μ oriented and ordered circles into the plane, whose singularities are only transverse double points. Such double points are divided into *classical crossings* and *virtual crossings*. At a classical crossing, we distinguish two intersecting arcs, called the *over-arc* and *under-arc* formally, by removing a small path from the under-arc to indicate the crossing information. We also define the *sign* of a classical crossing with respect to the orientation of the arcs as shown in the left of Figure 2.1. At a virtual crossing, we surround it by a small circle. See the right of the figure.

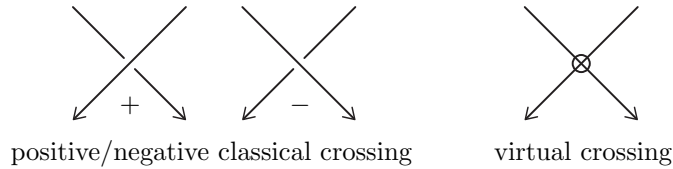


FIGURE 2.1. Two types of crossings

A μ -component virtual link is an equivalence class of μ -component virtual link diagrams under seven kinds of *generalized Reidemeister moves* R1–R3 and V1–V4 as shown in Figure 2.2 (cf. [5]). In particular, the moves R1–R3 are called *classical Reidemeister moves*, and V1–V4 are *virtual Reidemeister moves*. We remark that the equivalence relation keeps the order of the components. For example, Figure 2.3 shows a sequence of 2-component virtual link diagrams related by generalized Reidemeister moves five times.

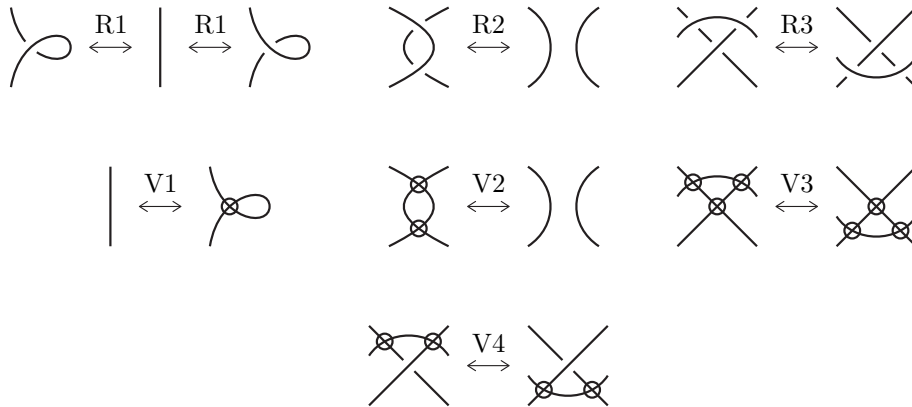


FIGURE 2.2. Generalized Reidemeister moves

A *Gauss diagram* is a disjoint union of ordered and oriented circles together with signed and oriented chords whose endpoints lie disjointly on the circles. A chord in a Gauss diagram is called a *self-chord* if both endpoints of the chord lie on the same circle of the Gauss diagram; otherwise it is called a *nonself-chord*. We say that a self-chord γ is *free* if the endpoints of γ are adjacent on the circle; that is, one of the arcs on the circle spanned by the endpoints of γ contains no endpoints of any other chords. Given a μ -component virtual link diagram D with n classical

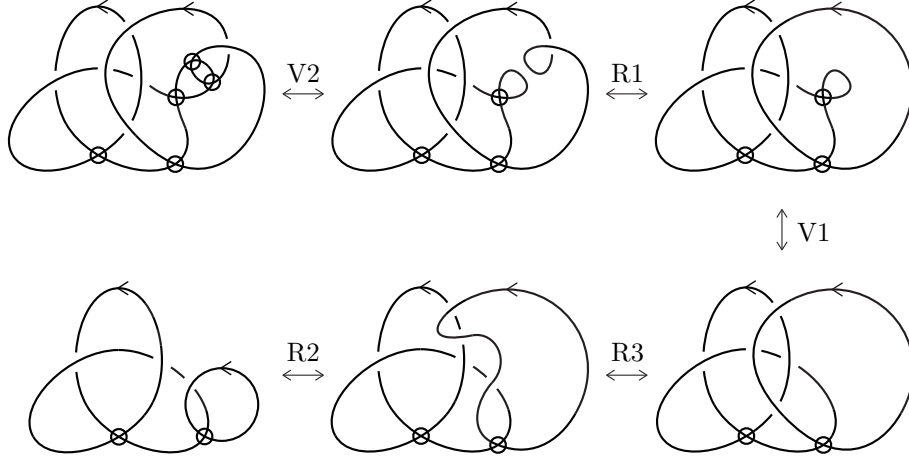


FIGURE 2.3. A sequence of 2-component virtual link diagrams

crossings and some or no virtual crossings, the *Gauss diagram associated with D* is defined to be the union of μ circles corresponding to the components of D and n chords connecting the preimage of each classical crossing. Each chord of the Gauss diagram is equipped with the sign of the corresponding classical crossing, and oriented from the over-arc to the under-arc.

Example 2.1. Let $L = K_1 \cup K_2$ be a 2-component virtual link presented by a virtual link diagram as shown in the left of Figure 2.4. The corresponding Gauss diagram consists of two circles C_1 and C_2 with six chords, where C_i corresponds to K_i ($i = 1, 2$). Three of the chords are self-chords corresponding to the crossings labeled 1, 2, and 6. In particular, the self-chord 6 is a free chord. The other three chords labeled 3, 4, and 5 are nonself-chords connecting the two circles C_1 and C_2 .

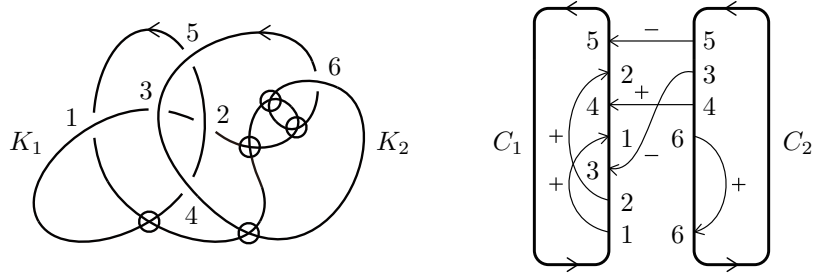


FIGURE 2.4. A 2-component virtual link diagram and its Gauss diagram

We consider the deformations on Gauss diagrams corresponding to generalized Reidemeister moves on virtual link diagrams. By definition, the four virtual Reidemeister moves V1–V4 on virtual link diagrams do not affect the corresponding Gauss diagrams; in fact, a Gauss diagram has no information on virtual crossings. On the other hand, a classical Reidemeister move R1 adds or removes a free chord in the corresponding Gauss diagram. See the left of Figure 2.5, where $\varepsilon = \pm$. For a classical Reidemeister move R2, we have an addition or deletion of a pair of chords with the same direction and opposite signs such that their initial and terminal endpoints are adjacent, respectively. See the right of the figure.

A classical Reidemeister move R3 involves three arcs and three classical crossings on a virtual link diagram. There are several types of R3's depending on the

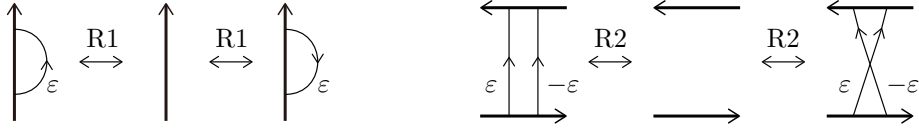


FIGURE 2.5. Reidemeister moves R1 and R2 on Gauss diagrams

orientations of the arcs and the over/under information at the crossings. Figure 2.6 shows two typical examples of Reidemeister moves R3 and the corresponding deformations on Gauss diagrams. We will use these two R3's in Section 5. Therefore a virtual link can be considered as an equivalence class of all Gauss diagrams under Reidemeister moves R1–R3 (cf. [3, 5]).

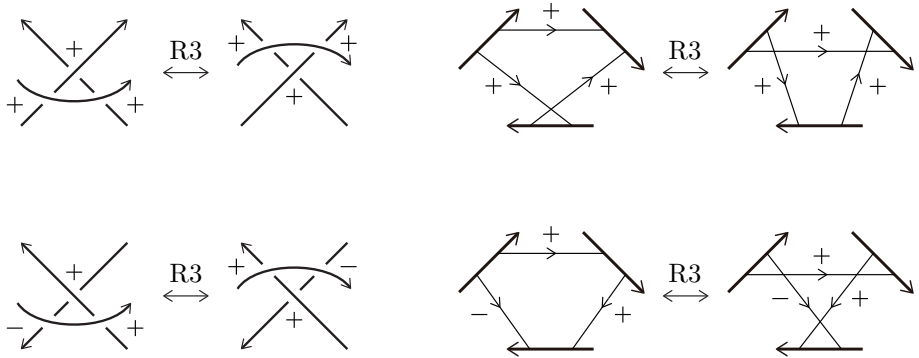


FIGURE 2.6. Two Reidemeister moves R3

Now we introduce another deformation on a Gauss diagram. Let P_1, P_2 , and P_3 be three consecutive endpoints of chords lying on the same circle of a Gauss diagram. A Ξ -move [13] is a deformation which exchanges the positions of P_1 and P_3 with preserving the signs and orientations of the chords. See Figure 2.7. In the definition of a Ξ -move, we consider all signs and orientations of the chords, and some of the chords are possibly the same. In the figure, a pair of dots \bullet marks the two endpoints P_1 and P_3 exchanged by a Ξ -move.

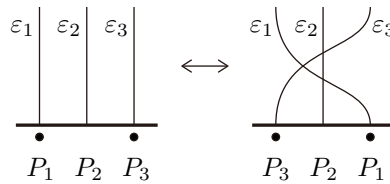


FIGURE 2.7. A Ξ -move

We say that two Gauss diagrams G and G' are Ξ -equivalent if they are related by a finite sequence of Reidemeister moves R1–R3 and Ξ -moves. We denote it by $G \sim G'$. Two virtual links are Ξ -equivalent if their Gauss diagrams are Ξ -equivalent.

In the rest of this paper, we only consider 2-component virtual links. Let $L = K_1 \cup K_2$ be a 2-component virtual link, and G a Gauss diagram presenting L with two circles C_1 and C_2 corresponding to the components K_1 and K_2 of L , respectively. For integers i and j with $\{i, j\} = \{1, 2\}$, a chord in G is called of type (i, j) if it is a nonself-chord connecting C_i and C_j and oriented from C_i to C_j .

Definition 2.2 (cf. [3, Section 1.7]). For i and j with $\{i, j\} = \{1, 2\}$, the (i, j) -linking number of $L = K_1 \cup K_2$ is the sum of signs of all nonself-chords of type (i, j) in G . We denote it by $\text{Lk}(K_i, K_j)$.

The integers $\text{Lk}(K_1, K_2)$ and $\text{Lk}(K_2, K_1)$ are both invariants of the virtual link L ; that is, they do not depend on a particular choice of a Gauss diagram G presenting L .

Definition 2.3 (cf. [7]). The *parity* of a 2-component virtual link $L = K_1 \cup K_2$ is the parity of $\text{Lk}(K_1, K_2) + \text{Lk}(K_2, K_1)$.

By definition, the parity of L is coincident with that of the number of nonself-chords in any Gauss diagram of L . For example, the 2-component virtual link $L = K_1 \cup K_2$ given in Example 2.1 satisfies $\text{Lk}(K_1, K_2) = 0$ and $\text{Lk}(K_2, K_1) = -1$, and therefore, L is odd.

We have a relationship between a Ξ -move and linking numbers as follows.

Lemma 2.4. *The (i, j) -linking number $\text{Lk}(K_i, K_j)$ of $L = K_1 \cup K_2$ is invariant under Ξ -moves for $\{i, j\} = \{1, 2\}$. Therefore the parity of L is preserved under Ξ -moves.*

Proof. For any nonself-chord in a Gauss diagram, a Ξ -move does not change its sign and type (i, j) . Therefore the sum of signs of all nonself-chords of type (i, j) is preserved. \square

3. PROOF OF THEOREM 1.2

In this section, we study 2-component *odd* virtual links, and prove Theorem 1.2 by giving a complete representative system of Ξ -equivalence classes of the links.

Lemma 3.1. *A deformation on a Gauss diagram as shown in Figure 3.1 is realized by two Ξ -moves.*

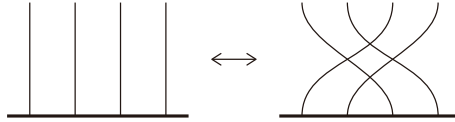


FIGURE 3.1. A deformation in Lemma 3.1

Proof. We apply a Ξ -move to the first and third endpoints, and another Ξ -move to the second and fourth endpoints. \square

Lemma 3.2. *A deformation on a Gauss diagram of a 2-component odd virtual link as shown in Figure 3.2 is realized by a finite number of Ξ -moves.*

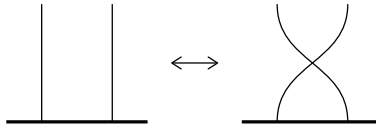


FIGURE 3.2. A deformation in Lemma 3.2

Proof. We may prove this lemma for two consecutive endpoints on the circle C_1 of the Gauss diagram. Since the virtual link is odd, the number of endpoints of chords on C_1 is odd. Let $P_1, P_2, \dots, P_{2n+1}$ be the endpoints on C_1 arranged in this order.

The exchange of the positions of P_1 and P_2 is realized by a combination of Ξ -moves as shown in Figure 3.3(1)–(4). More precisely, the arrangement (2) is obtained from (1) by applying the deformations in Lemma 3.1 $n - 1$ times. Next we obtain (3) from (2) by a single Ξ -move exchanging the positions of P_1 and P_{2n+1} . Finally we slide P_1 and P_2 along C_1 to obtain (4) from (3). \square

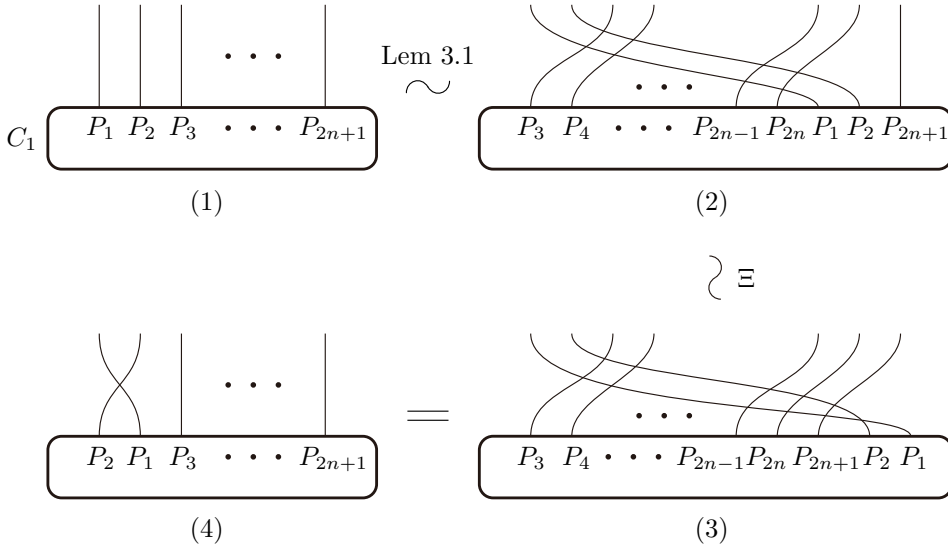


FIGURE 3.3. Proof of Lemma 3.2

We define a map $e : \mathbb{Z} \rightarrow \{-1, 0, 1\}$ by $e(n) = 1$ for $n > 0$, $e(n) = -1$ for $n < 0$, and $e(n) = 0$ for $n = 0$. For integers $a, b \in \mathbb{Z}$, we denote by $G(a, b)$ the Gauss diagram with two circles C_1 and C_2 as shown in the left of Figure 3.4; that is, it consists of $|a|$ horizontal nonself-chords of type (1, 2) with sign $e(a)$ and $|b|$ horizontal nonself-chords of type (2, 1) with sign $e(b)$. In the right of the figure, we illustrate the Gauss diagram $G(3, -2)$. Let $L(a, b)$ denote the 2-component virtual link presented by the Gauss diagram $G(a, b)$. Then we see that the set

$$\{L(a, b) \mid a, b \in \mathbb{Z} \text{ with } a + b \equiv 1 \pmod{2}\}$$

is a complete representative system of Ξ -equivalence classes of 2-component odd virtual links as follows.

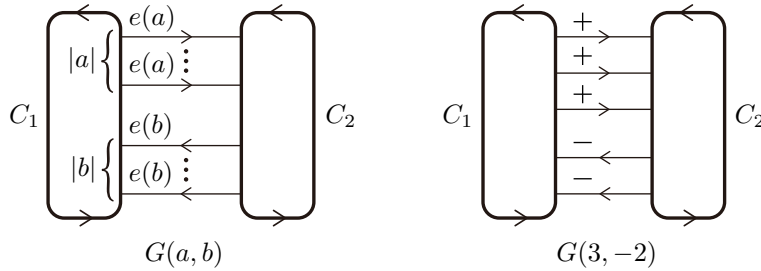


FIGURE 3.4. The Gauss diagram $G(a, b)$

Proposition 3.3. *Let $L = K_1 \cup K_2$ be a 2-component odd virtual link. Then L is Ξ -equivalent to $L(a, b)$, where $a = \text{Lk}(K_1, K_2)$ and $b = \text{Lk}(K_2, K_1)$.*

Proof. Let G be a Gauss diagram of L with two circles C_1 and C_2 . By Lemma 3.2, we can freely move the positions of endpoints on C_i ($i = 1, 2$) up to Ξ -equivalence. Therefore we deform every self-chord into a free chord, and remove it by an R1-move. Furthermore, we rearrange the nonself-chords horizontally so that the nonself-chords of type $(1, 2)$ are placed above those of type $(2, 1)$. If two consecutive nonself-chords of the same type have opposite signs, then we delete them by an R2-move. Finally G is Ξ -equivalent to $G(a, b)$ for some $a, b \in \mathbb{Z}$. Therefore L is Ξ -equivalent to the virtual link $L(a, b)$ presented by $G(a, b)$.

By definition, $L(a, b) = K'_1 \cup K'_2$ satisfies $\text{Lk}(K'_1, K'_2) = a$ and $\text{Lk}(K'_2, K'_1) = b$. Since L and $L(a, b)$ are Ξ -equivalent, we have $\text{Lk}(K_1, K_2) = a$ and $\text{Lk}(K_2, K_1) = b$ by Lemma 2.4. \square

Proof of Theorem 1.2. (i) \Rightarrow (ii). This follows from Lemma 2.4 directly.

(ii) \Rightarrow (i). By Proposition 3.3, $L = K_1 \cup K_2$ and $L' = K'_1 \cup K'_2$ are Ξ -equivalent to $L(a, b)$ and $L(a', b')$, respectively, where

$$a = \text{Lk}(K_1, K_2), \quad b = \text{Lk}(K_2, K_1), \quad a' = \text{Lk}(K'_1, K'_2), \quad \text{and} \quad b' = \text{Lk}(K'_2, K'_1).$$

Since $\text{Lk}(K_i, K_j) = \text{Lk}(K'_i, K'_j)$ holds for $\{i, j\} = \{1, 2\}$, we have $a = a'$ and $b = b'$. Therefore $L(a, b)$ is coincident to $L(a', b')$. \square

Remark 3.4. The deformation in Lemma 3.2 is called a *forbidden move* (cf. [3, 4, 10]). Lemma 3.2 implies that for a 2-component odd virtual link, a forbidden move is realized by Ξ -moves. On the other hand, a Ξ -move is obviously realized by forbidden moves. Therefore the classification of 2-component odd virtual links up to Ξ -moves is coincident with that up to forbidden moves, which is studied in [1, Proposition 3.6] and [12, Corollary 7].

4. SHELLS

To prove Theorem 1.3 for 2-component even virtual links, we prepare several lemmas and propositions in Sections 4 and 5. It is not necessary to restrict the argument to 2-component even virtual links. Therefore we do not assume that a 2-component virtual link is even in these sections.

In a Gauss diagram, let P_1, P_2 , and P_3 be three consecutive endpoints of chords lying on the same circle of the Gauss diagram. If P_1 and P_3 are connected by a self-chord, then the chord is called a *shell* (cf. [8]). See the left of Figure 4.1. Note that the orientation of a shell can be altered by a Ξ -move as shown in the right of the figure. In this sense, we may omit the orientation of a shell up to Ξ -equivalence in figures.

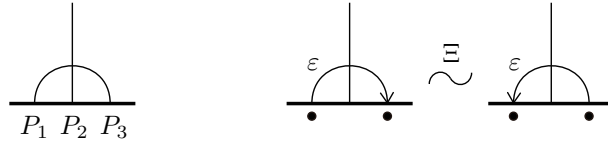


FIGURE 4.1. A shell and its orientation

A *shell-pair* consists of a pair of shells whose four endpoints are consecutive on the same circle. If a shell-pair consists of one positive and one negative shells, then we can delete it by an R2-move (after choosing the orientations of the shells suitably). We say that a shell-pair is *positive* (resp. *negative*) if it consists of two positive (resp. two negative) shells. See Figure 4.2.

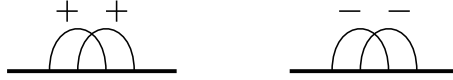


FIGURE 4.2. A positive/negative shell-pair

The following lemma allows us to move a shell-pair along a circle of a Gauss diagram freely.

Lemma 4.1. *If two Gauss diagrams are related by a deformation as shown in Figure 4.3, then they are Ξ -equivalent.*

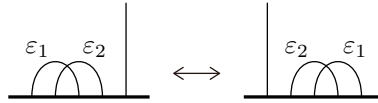


FIGURE 4.3. Moving a shell-pair along a circle

Proof. This follows by the deformation as shown in Figure 4.4. □

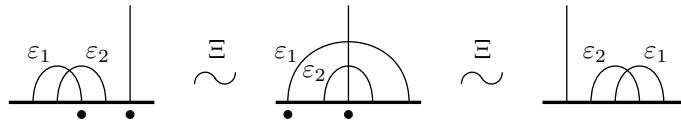


FIGURE 4.4. Proof of Lemma 4.1

A pair of positive and negative shell-pairs can be canceled in the following sense.

Lemma 4.2 (cf. [13, Fig. 13]). *If two Gauss diagrams are related by a deformation as shown in Figure 4.5, then they are Ξ -equivalent.*

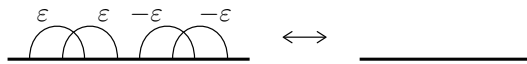


FIGURE 4.5. Adding/canceling two consecutive shell-pairs with opposite signs

Proof. This follows by the deformation as shown in Figure 4.6. □

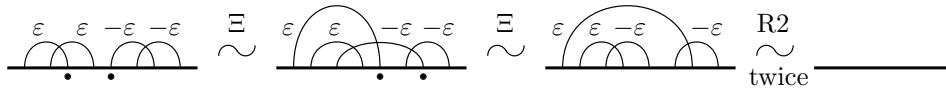


FIGURE 4.6. Proof of Lemma 4.2

We can exchange adjacent endpoints of chords (by ignoring shells) in the following sense.

Lemma 4.3. *If two Gauss diagrams are related by a deformation (1), (2), or (3) as shown in Figure 4.7, then they are Ξ -equivalent.*

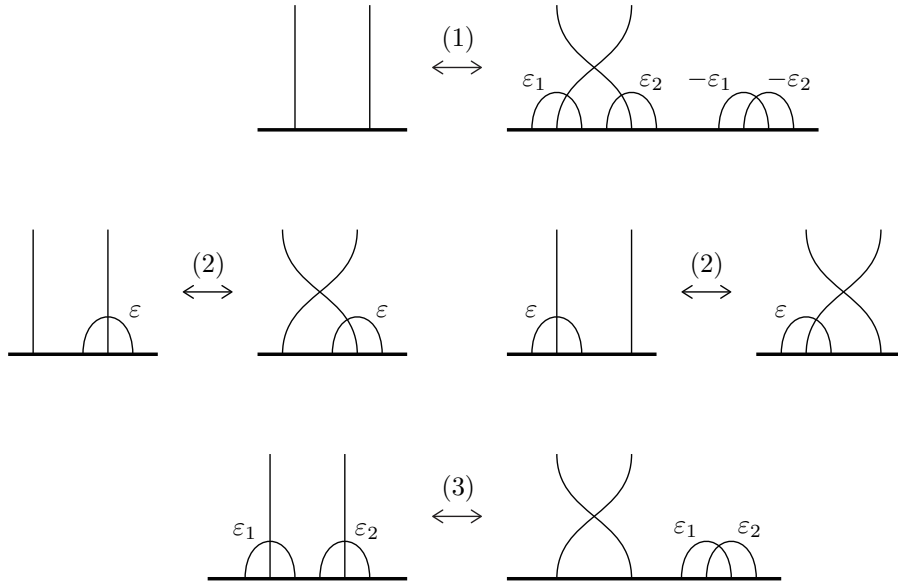


FIGURE 4.7. Deformations (1)–(3) in Lemma 4.3

Proof. (3) This is realized by two Ξ -moves as shown in Figure 4.8.

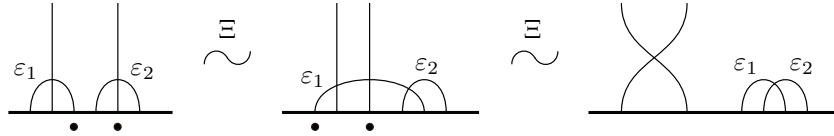


FIGURE 4.8. Proof of Lemma 4.3(3)

(1) This is obtained by (3) and Lemma 4.2 for $\varepsilon_1 = \varepsilon_2$, and by (3) and two R2-moves for $\varepsilon_1 = -\varepsilon_2$.

(2) This is realized by a single Ξ -move. \square

Lemma 4.4. *If two Gauss diagrams are related by a deformation as shown in Figure 4.9, then they are Ξ -equivalent.*



FIGURE 4.9. A deformation in Lemma 4.4

Proof. This follows by the deformation as shown in Figure 4.10. \square

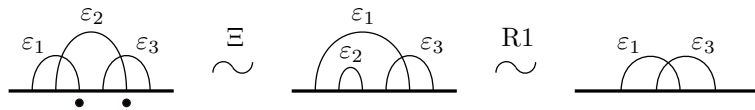


FIGURE 4.10. Proof of Lemma 4.4

Proposition 4.5. *Any Gauss diagram of a 2-component virtual link is Ξ -equivalent to a Gauss diagram with two circles C_1 and C_2 which satisfies the following conditions.*

- (i) *Any self-chord on C_i is a shell ($i = 1, 2$).*
- (ii) *All nonself-chords are arranged horizontally such that the nonself-chords of type (1, 2) are placed above those of type (2, 1).*

Figure 4.11 shows an example of a Gauss diagram satisfying the conditions (i) and (ii) in Proposition 4.5. We remark that any self-chord is either located around an endpoint of some nonself-chord or forms a shell-pair by the conditions.

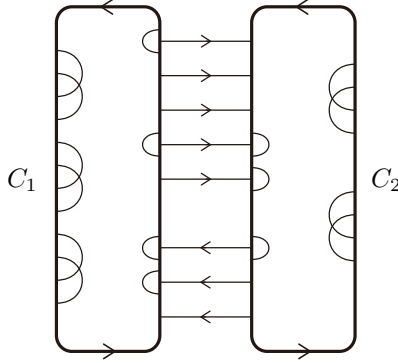


FIGURE 4.11. A Gauss diagram satisfying Proposition 4.5

Proof of Proposition 4.5. In a given Gauss diagram, let $\gamma_1, \dots, \gamma_n$ be all self-chords on C_1 , and let P_i and Q_i be the endpoints of γ_i ($i = 1, \dots, n$).

We first slide P_1 to Q_1 along the circle C_1 by using the deformations (1) and (2) in Lemma 4.3 as follows (see also Figure 4.12). Let X_1, \dots, X_s be the endpoints of self-/nonself-chords between P_1 and Q_1 lying in this order. First we exchange the positions of P_1 and X_1 by using the deformation (1) which adds a shell at P_1 , a shell at X_1 , and a shell-pair on C_1 . We may ignore the position of the shell-pair up to Ξ -equivalence by Lemma 4.1, and omit it in Figure 4.12. Next we exchange the positions of P_1 and X_2 by the deformation (2), which removes the shell at P_1 and adds a shell at X_2 . By applying the deformations (1) and (2) alternately to exchange P_1 and X_i ($i = 3, \dots, s$), γ_1 is finally deformed into a free chord if s is even, or it forms a shell-pair if s is odd. For s even, we remove γ_1 by an R1-move. γ_1 may be deformed into a self-chord that is not a shell.

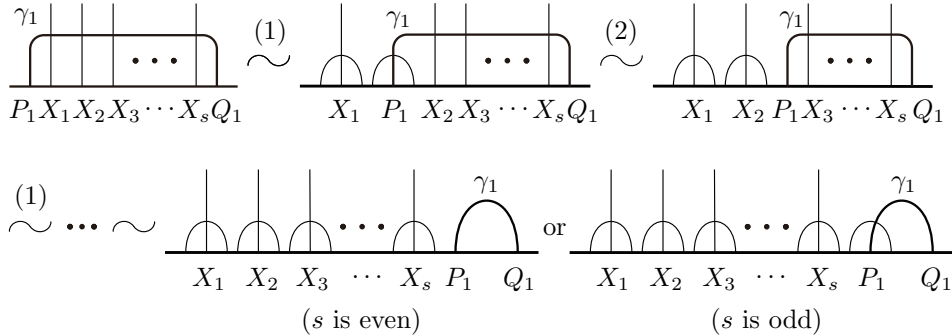


FIGURE 4.12. Sliding P_1 to Q_1 along C_1

In the obtained Gauss diagram, let Y_1, \dots, Y_t be the endpoints of chords between P_2 and Q_2 except for the endpoints of shells produced in the above sliding process of P_1 to Q_1 . Similarly to the sliding of P_1 to Q_1 , we slide P_2 to Q_2 along C_1 by exchanging P_2 and Y_1, \dots, Y_t step by step. Since P_2, Q_2 , and Y_i may have shells, we shall use the deformation (3) in Lemma 4.3 in addition to the deformations (1) and (2) as follows. If both P_2 and Y_i have shells for some i , we exchange their positions by using the deformation (3). This removes the shells at P_2 and at Y_i , and adds a shell-pair on C_1 . Likewise, if P_2 has no shell but Y_i does (resp. both P_2 and Y_i have no shells) for some i , we exchange their positions by using the deformation (2) (resp. deformation (1)). Applying this sliding process of P_2 to Q_2 leads to four cases depending on the number of shells at P_2 and Q_2 as shown in Figure 4.13. In the first case of the figure, γ_2 is a free chord and we remove it by an R1-move. In the second and third cases, we have a shell-pair. In the last case, we use Lemma 4.4 to obtain a shell-pair. For example, we consider the case $t = 5$ such that P_2, Q_2, Y_1, Y_2 , and Y_3 have shells as shown in the top-left of Figure 4.14. By the sliding process of P_2 to Q_2 , the self-chord γ_2 is deformed into the third cases of Figure 4.13 by applying the deformations (3), (2), (3), (1), and (2) in this order. Furthermore, Y_1, Y_2 , and Y_3 lose the shells, and Y_4 and Y_5 get shells.

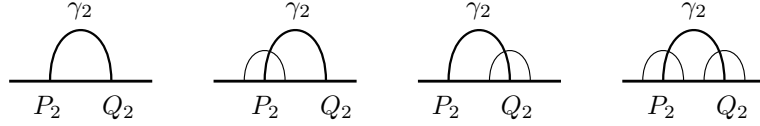
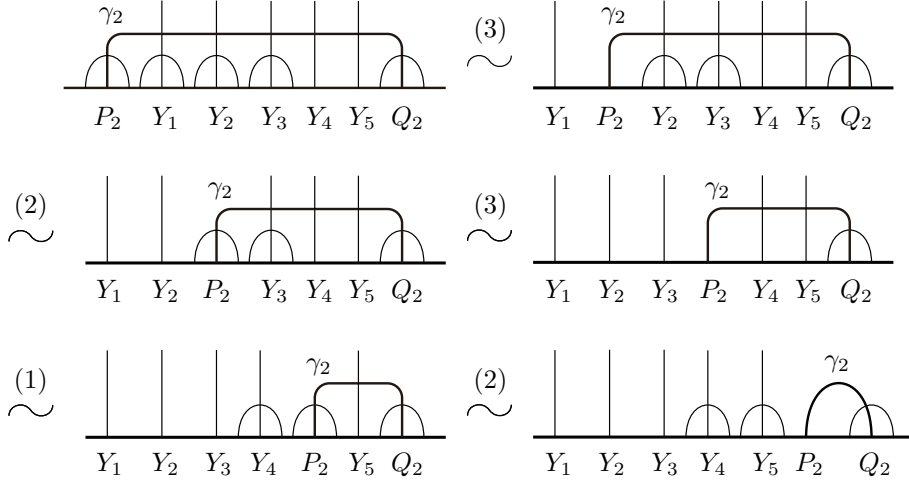


FIGURE 4.13. Four possible cases

FIGURE 4.14. An example of the sliding process of P_2 to Q_2

We slide P_i to Q_i for $i = 3, \dots, n$ similarly to the case $i = 2$ to obtain a Gauss diagram where any self-chord on C_1 is a shell. We perform a similar deformation for the self-chords on C_2 to obtain a Gauss diagram satisfying the condition (i).

Similarly to the deformations of self-chords as above, we deform the nonself-chords by Lemma 4.3 so that the obtained Gauss diagram satisfies the condition (ii) in addition to (i). \square

5. LADDERS

In this section, we introduce the notion of ladders and give a representative of the Ξ -equivalence class of a 2-component virtual link (Proposition 5.12).

The sign of a shell can be altered with making a shell-pair as follows.

Lemma 5.1. *If two Gauss diagrams are related by a deformation as shown in Figure 5.1, then they are Ξ -equivalent.*

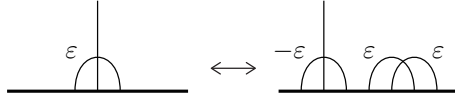


FIGURE 5.1. Altering the sign of a shell with a shell-pair

Proof. This follows by the deformation as shown in Figure 5.2. □

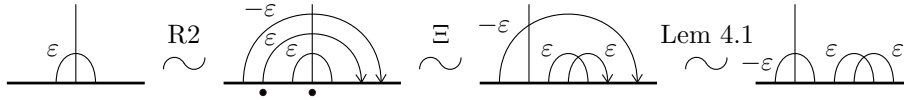


FIGURE 5.2. Proof of Lemma 5.1

By Lemmas 4.1 and 5.1, we may ignore the signs of shells and the positions of shell-pairs up to Ξ -equivalence, and we will often omit them in figures in the rest of this section.

We now consider a portion of a Gauss diagram consisting of two parallel arcs on C_1 and C_2 such that C_1 is oriented upwards and C_2 is oriented downwards together with horizontal nonself-chords of type $(1, 2)$ possibly with shells. Such a portion of the Gauss diagram is called a $(1, 2)$ -ladder. Figure 5.3 shows an example of a $(1, 2)$ -ladder with five nonself-chords.

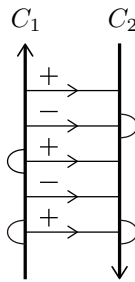
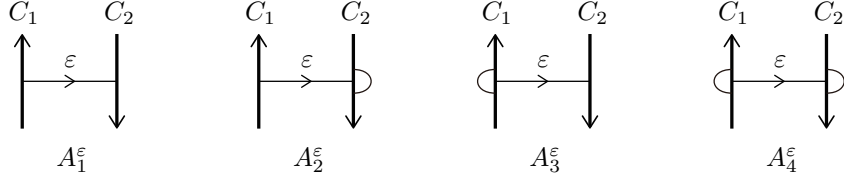


FIGURE 5.3. The $(1, 2)$ -ladder $A_1 A_2^{-1} A_3 A_1^{-1} A_4$

In a $(1, 2)$ -ladder, the nonself-chords of type $(1, 2)$ are divided into eight classes labeled $A_1^\varepsilon, A_2^\varepsilon, A_3^\varepsilon,$ and A_4^ε ($\varepsilon = \pm 1$) as shown in Figure 5.4, where ε is the sign of a nonself-chord. More precisely, a chord labeled A_1^{+1} or A_1^{-1} has no shells. On the other hand, a chord labeled A_2^{+1} or A_2^{-1} (resp. A_3^{+1} or A_3^{-1}) has a shell at the endpoint on C_2 (resp. C_1), and a chord labeled A_4^{+1} or A_4^{-1} has a pair of shells at both endpoints. Then the word on the letters $\{A_1, A_2, A_3, A_4\}$ of a $(1, 2)$ -ladder is obtained by reading the labels of nonself-chords in the ladder from top to bottom. For example, the $(1, 2)$ -ladder in Figure 5.3 is expressed by $A_1 A_2^{-1} A_3 A_1^{-1} A_4$, where

FIGURE 5.4. The labels $A_1^\varepsilon, A_2^\varepsilon, A_3^\varepsilon$ and A_4^ε of nonself-chords of type $(1, 2)$

we abbreviate X^{+1} to X simply for $X = A_1, A_2, A_3, A_4$. In what follows, we identify a $(1, 2)$ -ladder and its word on $\{A_1, A_2, A_3, A_4\}$.

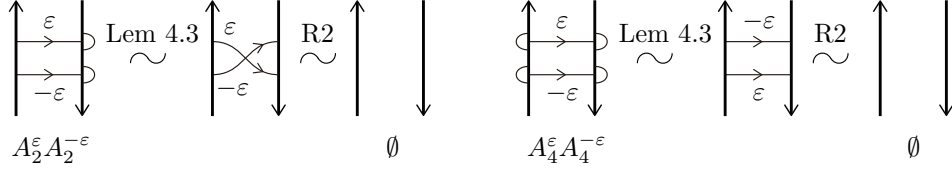
We study the Ξ -equivalence classes of $(1, 2)$ -ladders in Lemmas 5.2–5.5. Let \emptyset denote the empty word expressing the ladder with no chord. We remark that the product of \emptyset and any word W on $\{A_1, A_2, A_3, A_4\}$ is equal to W itself by definition.

Lemma 5.2. *For $i \in \{1, 2, 3, 4\}$, we have the Ξ -equivalence*

$$A_i A_i^{-1} \sim A_i^{-1} A_i \sim \emptyset$$

up to shell-pairs.

Proof. If $i = 1$, then $A_1 A_1^{-1}$ and $A_1^{-1} A_1$ are related to \emptyset by R2-moves. Figure 5.5 shows the proofs for $i = 2, 4$. The proof for $i = 3$ is similar to that for $i = 2$. \square

FIGURE 5.5. Proofs of Lemma 5.2 for $i = 2, 4$

By Lemma 5.2, if two words W and V on $\{A_1, A_2, A_3, A_4\}$ satisfy $WV \sim \emptyset$, then we have

$$W \sim W(VV^{-1}) \sim (WV)V^{-1} \sim V^{-1}$$

and $V \sim W^{-1}$, where W^{-1} and V^{-1} are the inverse words of W and V , respectively. We remark that the Ξ -equivalence class of any $(1, 2)$ -ladder up to shell-pairs by an element of the free group generated by $\{A_1, A_2, A_3, A_4\}$.

Lemma 5.3. *We have the following Ξ -equivalence up to shell-pairs.*

- (i) $A_1 A_2 \sim A_2 A_1 \sim A_3 A_4 \sim A_4 A_3$.
- (ii) $A_1 A_3 \sim A_3 A_1 \sim A_2 A_4 \sim A_4 A_2$.
- (iii) $A_1 A_4 \sim A_4 A_1$ and $A_2 A_3 \sim A_3 A_2$.

In particular, the letters A_1, A_2, A_3 , and A_4 are mutually commutative.

Proof. (i) Figure 5.6 shows the proof. We remark that the R3-move in the figure is the same as the one used at the top of Figure 2.6.

(ii) The proof is similar to that of (i) by exchanging A_2 and A_3 .

(iii) It holds that $A_4 \sim A_3^{-1} A_2 A_1$ by $A_3 A_4 \sim A_2 A_1$ in (i) and Lemma 5.2, $A_1 A_3^{-1} \sim A_3^{-1} A_1$ by $A_1 A_3 \sim A_3 A_1$ in (ii), and $A_1 A_2 \sim A_2 A_1$ in (i). Therefore we have

$$\begin{aligned} A_1 A_4 &\sim A_1 (A_3^{-1} A_2 A_1) = (A_1 A_3^{-1}) A_2 A_1 \sim (A_3^{-1} A_1) A_2 A_1 \\ &= A_3^{-1} (A_1 A_2) A_1 \sim A_3^{-1} (A_2 A_1) A_1 = (A_3^{-1} A_2 A_1) A_1 \sim A_4 A_1. \end{aligned}$$

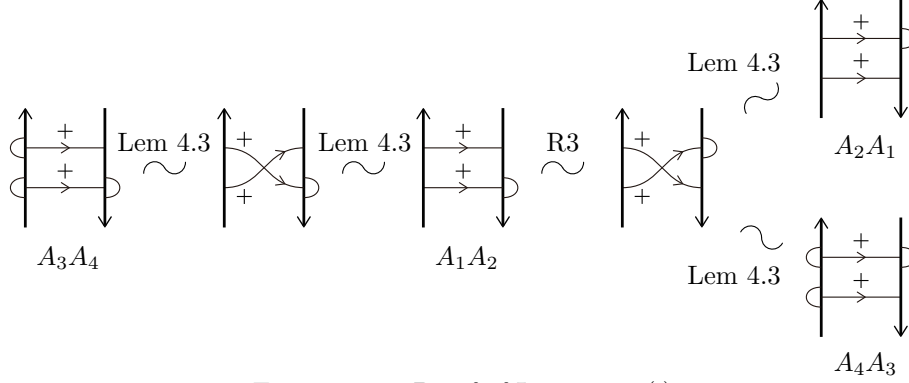


FIGURE 5.6. Proof of Lemma 5.3(i)

Similarly, it holds that $A_3 \sim A_4^{-1}A_1A_2$ by $A_4A_3 \sim A_1A_2$ in (i), $A_2A_4^{-1} \sim A_4^{-1}A_2$ by $A_2A_4 \sim A_4A_2$ in (ii), and $A_1A_2 \sim A_2A_1$ in (i). Therefore we have

$$A_2A_3 \sim A_2A_4^{-1}A_1A_2 \sim A_4^{-1}A_2A_1A_2 \sim A_4^{-1}A_1A_2A_2 \sim A_3A_2.$$

□

Lemma 5.4. *We have the Ξ -equivalence $A_2^2 \sim A_3^2$ up to shell-pairs.*

Proof. This follows by the deformation as shown in Figure 5.7. □

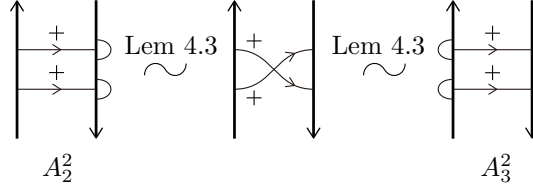


FIGURE 5.7. Proof of Lemma 5.4

Lemma 5.5. *Any (1, 2)-ladder is Ξ -equivalent to either $A_1^{a_1}A_2^{a_2}$ or $A_1^{a_1}A_2^{a_2}A_3$ for some $a_1, a_2 \in \mathbb{Z}$ up to shell-pairs.*

Proof. By Lemmas 5.2, 5.3, and 5.4, the Ξ -equivalence class of any (1, 2)-ladder up to shell-pairs is regarded as an element in the abelian group presented by

$$\left\langle A_1, A_2, A_3, A_4 \mid \begin{array}{l} A_iA_j = A_jA_i \ (1 \leq i < j \leq 4), \\ A_1A_2 = A_3A_4, \ A_1A_3 = A_2A_4, \ A_2^2 = A_3^2 \end{array} \right\rangle.$$

Since this group is isomorphic to

$$\langle A_1, A_2, A_3 \mid A_iA_j = A_jA_i \ (1 \leq i < j \leq 3), \ A_2^2 = A_3^2 \rangle \cong \mathbb{Z} \times \mathbb{Z} \times (\mathbb{Z}/2\mathbb{Z}),$$

we have the conclusion. □

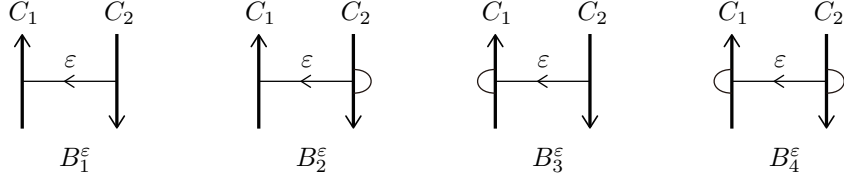
Similarly to a (1, 2)-ladder, we define a (2, 1)-ladder as a portion consisting of nonself-chords of type (2, 1), which are labeled B_1^ε , B_2^ε , B_3^ε , and B_4^ε ($\varepsilon = \pm 1$) as shown in Figure 5.8. Then we have similar properties to Lemmas 5.2–5.5 as follows.

Lemma 5.6. *For $i \in \{1, 2, 3, 4\}$, we have the Ξ -equivalence*

$$B_iB_i^{-1} \sim B_i^{-1}B_i \sim \emptyset$$

up to shell-pairs. □

Lemma 5.7. *We have the following Ξ -equivalence up to shell-pairs.*

FIGURE 5.8. The labels $B_1^\epsilon, B_2^\epsilon, B_3^\epsilon$ and B_4^ϵ of nonself-chords of type $(2, 1)$

- (i) $B_1 B_2 \sim B_2 B_1 \sim B_3 B_4 \sim B_4 B_3$.
- (ii) $B_1 B_3 \sim B_3 B_1 \sim B_2 B_4 \sim B_4 B_2$.
- (iii) $B_1 B_4 \sim B_4 B_1$ and $B_2 B_3 \sim B_3 B_2$.

In particular, the letters B_1, B_2, B_3 , and B_4 are mutually commutative. \square

Lemma 5.8. We have the Ξ -equivalence $B_2^2 \sim B_3^2$ up to shell-pairs. \square

Lemma 5.9. Any $(2, 1)$ -ladder is Ξ -equivalent to either $B_1^{b_1} B_2^{b_2}$ or $B_1^{b_1} B_2^{b_2} B_3$ for some $b_1, b_2 \in \mathbb{Z}$ up to shell-pairs. \square

For a $(1, 2)$ -ladder W and a $(2, 1)$ -ladder V , we consider the ladder WV obtained by stacking W on top of V , as for example on the left-hand side of Figure 5.9. Then we have the following.

Lemma 5.10. We have the Ξ -equivalence $A_2 B_2 \sim A_3 B_3$ up to shell-pairs.

Proof. This follows by the deformation as shown in Figure 5.9. We remark that the R3-move in the figure is the same as the one used at the bottom of Figure 2.6. \square

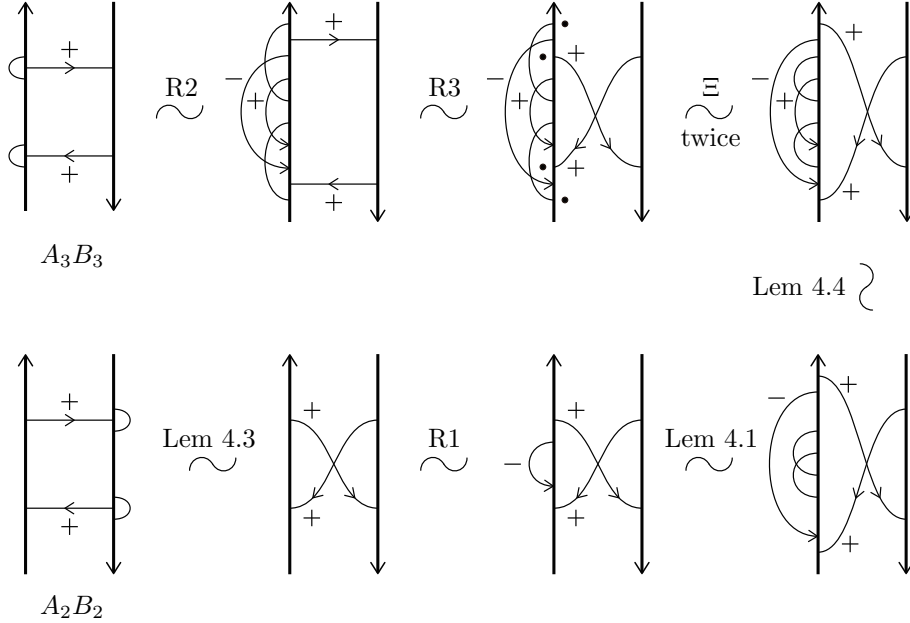


FIGURE 5.9. Proof of Lemma 5.10

Proposition 5.11. For a $(1, 2)$ -ladder W and a $(2, 1)$ -ladder V , the ladder WV is Ξ -equivalent to either

$$A_1^{a_1} A_2^{a_2} B_1^{b_1} B_2^{b_2} \text{ or } A_1^{a_1} A_2^{a_2} B_1^{b_1} B_2^{b_2} B_3$$

for some $a_1, a_2, b_1, b_2 \in \mathbb{Z}$ up to shell-pairs.

Proof. By Lemmas 5.5 and 5.9, we have

$$W \sim A_1^{a_1} A_2^{a_2} A_3^{a_3} \text{ and } V \sim B_1^{b_1} B_2^{b_2} B_3^{b_3}$$

for some $a_1, a_2, b_1, b_2 \in \mathbb{Z}$ and $a_3, b_3 \in \{0, 1\}$. For $a_3 = 0$, we have $WV \sim A_1^{a_1} A_2^{a_2} B_1^{b_1} B_2^{b_2} B_3^{b_3}$ which gives a conclusion.

Now we consider the case $a_3 = 1$. It holds that $A_3 \sim A_2 B_2 B_3^{-1}$ by Lemmas 5.6 and 5.10. Since B_1, B_2 , and B_3 commute mutually up to Ξ -equivalence by Lemma 5.7, we have

$$\begin{aligned} WV &\sim A_1^{a_1} A_2^{a_2} A_3 B_1^{b_1} B_2^{b_2} B_3^{b_3} \\ &\sim A_1^{a_1} A_2^{a_2} (A_2 B_2 B_3^{-1}) B_1^{b_1} B_2^{b_2} B_3^{b_3} \\ &\sim A_1^{a_1} A_2^{a_2+1} B_1^{b_1} B_2^{b_2+1} B_3^{b_3-1}. \end{aligned}$$

If $b_3 = 1$, then we have a conclusion. We consider the case $b_3 = 0$, that is, $WV \sim A_1^{a_1} A_2^{a_2+1} B_1^{b_1} B_2^{b_2+1} B_3^{-1}$. Since $B_3^{-1} \sim B_2^{-2} B_3$ holds by Lemma 5.8, we have

$$\begin{aligned} WV &\sim A_1^{a_1} A_2^{a_2+1} B_1^{b_1} B_2^{b_2+1} B_3^{-1} \\ &\sim A_1^{a_1} A_2^{a_2+1} B_1^{b_1} B_2^{b_2+1} (B_2^{-2} B_3) \\ &\sim A_1^{a_1} A_2^{a_2+1} B_1^{b_1} B_2^{b_2-1} B_3. \end{aligned}$$

□

For integers $a_1, a_2, b_1, b_2, k, l \in \mathbb{Z}$, we denote by

$$G(a_1, a_2, b_1, b_2; k, l) \text{ and } H(a_1, a_2, b_1, b_2; k, l)$$

the Gauss diagrams as shown in Figure 5.10. More precisely, their ladders are

$$A_1^{a_1} A_2^{a_2} B_1^{b_1} B_2^{b_2} \text{ and } A_1^{a_1} A_2^{a_2} B_1^{b_1} B_2^{b_2} B_3,$$

respectively, and all nonself-chords in $A_1^{a_1}$ (resp. $A_2^{a_2}$, $B_1^{b_1}$, and $B_2^{b_2}$) have the sign $e(a_1)$ (resp. $e(a_2)$, $e(b_1)$, and $e(b_2)$). Furthermore, there are $|k|$ shell-pairs with sign $e(k)$ on C_1 and $|l|$ shell-pairs with sign $e(l)$ on C_2 . We denote by

$$L(a_1, a_2, b_1, b_2; k, l) \text{ and } M(a_1, a_2, b_1, b_2; k, l)$$

the 2-component virtual links presented by the Gauss diagrams $G(a_1, a_2, b_1, b_2; k, l)$ and $H(a_1, a_2, b_1, b_2; k, l)$, respectively.

Proposition 5.12. *Any 2-component virtual link L is Ξ -equivalent to either*

$$L(a_1, a_2, b_1, b_2; k, l) \text{ or } M(a_1, a_2, b_1, b_2; k, l)$$

for some $a_1, a_2, b_1, b_2, k, l \in \mathbb{Z}$.

Proof. Any Gauss diagram of L is Ξ -equivalent to a Gauss diagram G_1 which satisfies the conditions (i) and (ii) in Proposition 4.5.

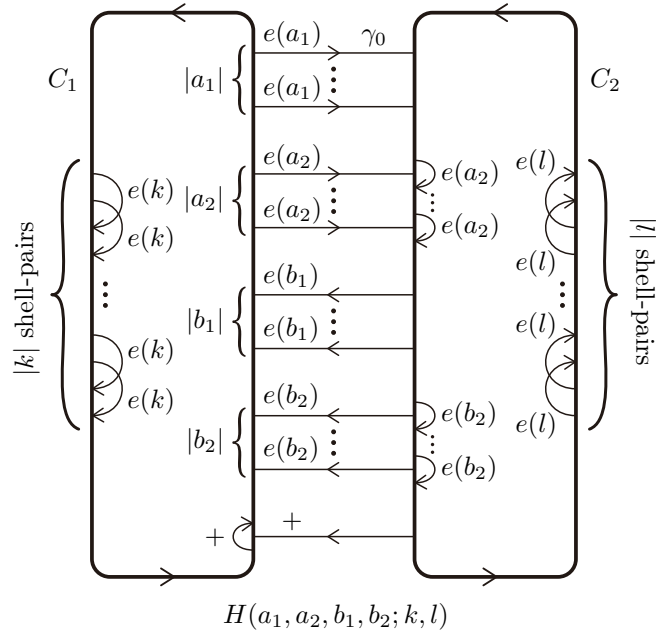
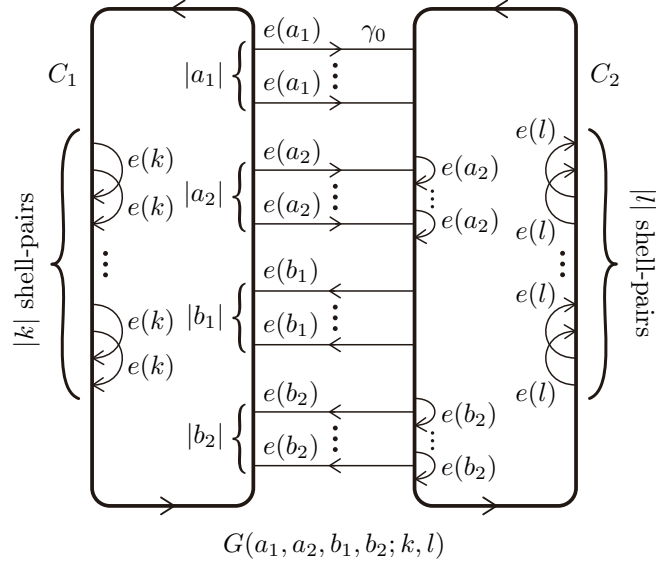
Let W and V be the (1, 2)- and (2, 1)-ladders of G_1 , respectively. By Proposition 5.11, the ladder WV is Ξ -equivalent to either

$$A_1^{a_1} A_2^{a_2} B_1^{b_1} B_2^{b_2} \text{ or } A_1^{a_1} A_2^{a_2} B_1^{b_1} B_2^{b_2} B_3$$

with producing a finite number of shell-pairs for some $a_1, a_2, b_1, b_2 \in \mathbb{Z}$. Let G_2 be the obtained Gauss diagram.

By Lemma 5.1, G_2 is Ξ -equivalent to a Gauss diagram G_3 such that any shell at an endpoint of a nonself-chord labeled A_2^{\pm} , B_2^{\pm} , or B_3 has the same sign as that of the nonself-chord. We may produce a finite number of shell-pairs in this Ξ -equivalence.

If a circle C_i ($i = 1, 2$) of G_3 has a shell-pair consisting of positive and negative shells, then we delete it by an R2-move. Furthermore, if C_i has a pair of positive and negative shell-pairs, then we cancel it by Lemmas 4.1 and 4.2. Let G_4 be the

FIGURE 5.10. $G(a_1, a_2, b_1, b_2; k, l)$ and $H(a_1, a_2, b_1, b_2; k, l)$

obtained Gauss diagram, where all shell-pairs in each C_i ($i = 1, 2$) have the same sign.

Recall that the orientation of a shell can be altered by a Ξ -move (without producing new shell-pairs). Therefore G_4 is Ξ -equivalent to a Gauss diagram G_5 such that the orientation of any shell on C_i is coherent to that of C_i ($i = 1, 2$) as in Figure 5.10. This Gauss diagram G_5 is coincident with $G(a_1, a_2, b_1, b_2; k, l)$ or $H(a_1, a_2, b_1, b_2; k, l)$ finally. \square

6. INVARIANTS OF A 2-COMPONENT EVEN VIRTUAL LINK

Throughout Sections 6 and 7, we consider a 2-component *even* virtual link $L = K_1 \cup K_2$ and its Gauss diagram G . In this section, we introduce three kinds of invariants $J(L, K_1)$, $J(L, K_2)$, and $\overline{F}(L)$ of L , and establish a relationship among these invariants (Theorem 6.10).

Let γ be a self-chord on a circle C_i of G . The endpoints of γ divide C_i into two arcs. Let α be one of the two arcs. We define the *parity* of γ to be the parity of the number of endpoints of self-/nonself-chords on α . Since the number of nonself-chords in G is even, the parity of γ does not depend on a particular choice of the arc α ; in fact, the number of endpoints of self-/nonself-chords on C_i ($i = 1, 2$) is even. By definition, any shell is odd. Let $J(G, C_i)$ denote the sum of signs of all odd self-chords on C_i .

Example 6.1. Consider the Gauss diagram $G = H(3, -2, 1, 1; -3, 2)$ as shown in Figure 6.1. Then the self-chords on C_1 consist of one positive shell and six negative shells, and those on C_2 consist of five positive shells and two negative shells. Therefore we have

$$J(G, C_1) = -5 \text{ and } J(G, C_2) = 3.$$

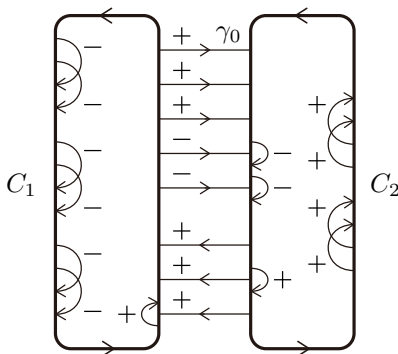


FIGURE 6.1. The Gauss diagram $H(3, -2, 1, 1; -3, 2)$

Lemma 6.2. *The integer $J(G, C_i)$ is an invariant of the 2-component even virtual link L for $i = 1, 2$. Furthermore, it is invariant under Ξ -moves.*

Proof. An R1-move adds or removes an even self-chord, and preserves the parity of any other self-chords. An R2-move adds or deletes a pair of chords γ and γ' with opposite signs, and preserves the parity of any other self-chords. If γ and γ' are nonself-chords, then they do not contribute to $J(G, C_i)$. If γ and γ' are self-chords on C_i , then they have the same parity and the contributions to $J(G, C_i)$ cancel out. An R3-move or a Ξ -move preserves the sign and parity of any self-chords. \square

Definition 6.3. The integer $J(G, C_i)$ is called the *odd writhe of the pair (L, K_i)* ($i = 1, 2$), and is denoted by $J(L, K_i)$.

For example, the virtual link $L = K_1 \cup K_2 = M(3, -2, 1, 1; -3, 2)$ presented by the Gauss diagram $H(3, -2, 1, 1; -3, 2)$ of Figure 6.1 has the odd writhes

$$J(L, K_1) = -5 \text{ and } J(L, K_2) = 3.$$

We stress that the odd writhe $J(L, K_i)$ of the pair (L, K_i) is different from the original odd writhe $J(K_i)$ of the virtual knot K_i itself introduced in [6], meaning that $J(L, K_i)$ is an invariant of L rather than K_i .

Fix a nonself-chord γ_0 in G . For any other nonself-chord γ in G , the endpoints of γ_0 and γ on C_1 divide the circle C_1 into two arcs. Let α be one of the two arcs. Similarly, the endpoints of γ_0 and γ on C_2 divide C_2 into two arcs, and let β be one of the two arcs. See Figure 6.2. We consider two sets of nonself-chords γ in G as follows;

$$S(\gamma_0) = \{\gamma \mid \text{the number of endpoints of chords on } \alpha \cup \beta \text{ is even}\}$$

and

$$T(\gamma_0) = \{\gamma \mid \text{the number of endpoints of chords on } \alpha \cup \beta \text{ is odd}\}.$$

As a convention, we set $\gamma_0 \in S(\gamma_0)$. Since the number of nonself-chords in G is even, the parity of the number of endpoints of chords on $\alpha \cup \beta$ does not depend on a particular choice of the arcs α and β . Therefore the sets $S(\gamma_0)$ and $T(\gamma_0)$ are well-defined for γ_0 .

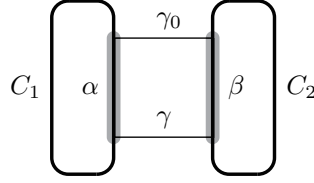


FIGURE 6.2. A pair of arcs α and β for nonself-chords γ_0 and γ

Let $\sigma_{12}(G, \gamma_0)$ and $\tau_{12}(G, \gamma_0)$ be the sums of signs of all nonself-chords of type $(1, 2)$ in $S(\gamma_0)$ and $T(\gamma_0)$, respectively. Similarly, let $\sigma_{21}(G, \gamma_0)$ and $\tau_{21}(G, \gamma_0)$ be the sums of signs of all nonself-chords of type $(2, 1)$ in $S(\gamma_0)$ and $T(\gamma_0)$, respectively. By definition, we have

$$\sigma_{12}(G, \gamma_0) + \tau_{12}(G, \gamma_0) = \text{Lk}(K_1, K_2) \text{ and } \sigma_{21}(G, \gamma_0) + \tau_{21}(G, \gamma_0) = \text{Lk}(K_2, K_1).$$

We introduce an equivalence relation \doteq among the elements in \mathbb{Z}^4 as follows. For two elements (a_1, a_2, b_1, b_2) and $(c_1, c_2, d_1, d_2) \in \mathbb{Z}^4$, we define $(a_1, a_2, b_1, b_2) \doteq (c_1, c_2, d_1, d_2)$ if and only if

$$(a_1, a_2, b_1, b_2) = (c_1, c_2, d_1, d_2) \text{ or } (c_2, c_1, d_2, d_1).$$

We denote by $[a_1, a_2, b_1, b_2]$ the equivalence class of (a_1, a_2, b_1, b_2) under the equivalence relation \doteq . For a nonself-chord γ_0 in G , we put

$$\overline{F}(G, \gamma_0) = [\sigma_{12}(G, \gamma_0), \tau_{12}(G, \gamma_0), \sigma_{21}(G, \gamma_0), \tau_{21}(G, \gamma_0)] \in \mathbb{Z}^4 / \doteq.$$

Example 6.4. Consider the Gauss diagram $G = H(3, -2, 1, 1; -3, 2)$ given in Example 6.1. The ladder of G is expressed by $A_1^3 A_2^{-2} B_1 B_2 B_3$. Let γ_0 be the top nonself-chord labeled A_1 as shown in Figure 6.1. Then the set $S(\gamma_0)$ consists of nonself-chords labeled A_1 or B_2 , and $T(\gamma_0)$ consists of those labeled A_2^{-1} , B_2 , or B_3 . Hence we have

$$\sigma_{12}(G, \gamma_0) = 3, \tau_{12}(G, \gamma_0) = -2, \sigma_{21}(G, \gamma_0) = 1, \text{ and } \tau_{21}(G, \gamma_0) = 2,$$

and it holds that $\overline{F}(G, \gamma_0) = [3, -2, 1, 2] = [-2, 3, 2, 1]$.

Lemma 6.5. *The equivalence class $\overline{F}(G, \gamma_0)$ is an invariant of the 2-component even virtual link L . Furthermore, it is invariant under Ξ -moves.*

Proof. We first prove that $\overline{F}(G, \gamma_0)$ does not depend on a particular choice of γ_0 . Consider a nonself-chord γ_1 in G . In the case $\gamma_1 \in S(\gamma_0)$, we have

$$\sigma_{ij}(G, \gamma_0) = \sigma_{ij}(G, \gamma_1) \text{ and } \tau_{ij}(G, \gamma_0) = \tau_{ij}(G, \gamma_1)$$

for $\{i, j\} = \{1, 2\}$. In the case $\gamma_1 \in T(\gamma_0)$, we have

$$\sigma_{ij}(G, \gamma_0) = \tau_{ij}(G, \gamma_1) \text{ and } \tau_{ij}(G, \gamma_0) = \sigma_{ij}(G, \gamma_1)$$

for $\{i, j\} = \{1, 2\}$. Therefore $\overline{F}(G, \gamma_0) = \overline{F}(G, \gamma_1)$ holds.

We can also prove that $\overline{F}(G, \gamma_0)$ is invariant under an R2-move adding a pair of nonself-chords. In fact, it leaves $\sigma_{ij}(G, \gamma_0)$ and $\tau_{ij}(G, \gamma_0)$ unchanged for $\{i, j\} = \{1, 2\}$.

Now we consider a Reidemeister move R1–R3 or Ξ -move on G generally. By using the above two properties if necessary, we may assume that such a move does not involve γ_0 . Then it can be seen that this move preserves $\sigma_{ij}(G, \gamma_0)$ and $\tau_{ij}(G, \gamma_0)$ for $\{i, j\} = \{1, 2\}$. \square

Definition 6.6. The equivalence class $\overline{F}(G, \gamma_0) \in \mathbb{Z}^4 / \doteq$ is called the *reduced linking class* of L , and is denoted by $\overline{F}(L)$.

Remark 6.7. There is an invariant of L called the *linking class* $F(L)$ (cf. [2, 8]). We can prove that the reduced linking class $\overline{F}(L)$ is obtained from $F(L)$. We do not give the definition of $F(L)$ in this paper, and leave the proof to the reader.

Now we have three kinds of invariants $J(L, K_1)$, $J(L, K_2)$, and $\overline{F}(L)$. To study a relationship among these invariants, we prepare the following two lemmas. Recall that $L(a_1, a_2, b_1, b_2; k, l)$ and $M(a_1, a_2, b_1, b_2; k, l)$ are the 2-component virtual links introduced at the end of Section 5.

Lemma 6.8. *Let $a_1, a_2, b_1, b_2, k, l \in \mathbb{Z}$. We have the following.*

(i) $L(a_1, a_2, b_1, b_2; k, l)$ is even if and only if

$$a_1 + a_2 + b_1 + b_2 \equiv 0 \pmod{2}.$$

(ii) $M(a_1, a_2, b_1, b_2; k, l)$ is even if and only if

$$a_1 + a_2 + b_1 + b_2 \equiv 1 \pmod{2}.$$

Proof. Recall that a 2-component virtual link is even if and only if the number of nonself-chords in its Gauss diagram is even. Since the numbers of nonself-chords in $G(a_1, a_2, b_1, b_2; k, l)$ and $H(a_1, a_2, b_1, b_2; k, l)$ are equal to

$$|a_1| + |a_2| + |b_1| + |b_2| \text{ and } |a_1| + |a_2| + |b_1| + |b_2| + 1,$$

respectively, we have the conclusion. \square

Lemma 6.9. *We have the following.*

(i) If $L = K_1 \cup K_2 = L(a_1, a_2, b_1, b_2; k, l)$ is even, then it holds that

$$J(L, K_1) = 2k, \quad J(L, K_2) = a_2 + b_2 + 2l, \text{ and } \overline{F}(L) = [a_1, a_2, b_1, b_2].$$

(ii) If $L = K_1 \cup K_2 = M(a_1, a_2, b_1, b_2; k, l)$ is even, then it holds that

$$J(L, K_1) = 2k + 1, \quad J(L, K_2) = a_2 + b_2 + 2l, \text{ and } \overline{F}(L) = [a_1, a_2, b_1, b_2 + 1].$$

Proof. Since the proofs of (i) and (ii) are similar, we only prove (ii).

We consider the Gauss diagram $G = H(a_1, a_2, b_1, b_2; k, l)$. Since any self-chord on each circle C_i ($i = 1, 2$) of G is odd, it contributes to $J(G, C_i)$. The sum of all self-chords on C_1 is equal to $2k + 1$, and that on C_2 is equal to $a_2 + b_2 + 2l$. Therefore we have

$$J(L, K_1) = J(G, C_1) = 2k + 1 \text{ and } J(L, K_2) = J(G, C_2) = a_2 + b_2 + 2l.$$

Recall that the ladder of G is $A_1^{a_1} A_2^{a_2} B_1^{b_1} B_2^{b_2} B_3$. Let γ_0 be the top nonself-chord in G labeled $A_1^{e(a_1)}$ as shown in Figure 5.10. Then the set $S(\gamma_0)$ consists of the nonself-chords labeled $A_1^{e(a_1)}$ or $B_1^{e(b_1)}$, and $T(\gamma_0)$ consists of those labeled $A_2^{e(a_2)}$,

$B_2^{e(b_2)}$, or B_3 . Since the sum of signs of all nonself-chords labeled $A_1^{e(a_1)}$ (resp. $B_1^{e(b_1)}$) is equal to a_1 (resp. b_1), we have

$$\sigma_{12}(G, \gamma_0) = a_1 \text{ and } \sigma_{21}(G, \gamma_0) = b_1.$$

Similarly, since the sum of signs of all nonself-chords labeled $A_2^{e(a_2)}$ (resp. $B_2^{e(b_2)}$ or B_3) is equal to a_2 (resp. $b_2 + 1$), we have

$$\tau_{12}(G, \gamma_0) = a_2 \text{ and } \tau_{21}(G, \gamma_0) = b_2 + 1.$$

Therefore $\overline{F}(L) = \overline{F}(G, \gamma_0) = [a_1, a_2, b_1, b_2 + 1]$ holds. \square

We establish a relationship among the invariants $J(L, K_1)$, $J(L, K_2)$, and $\overline{F}(L)$ of a 2-component even virtual link $L = K_1 \cup K_2$ as follows.

Theorem 6.10. *If $\overline{F}(L) = [a_1, a_2, b_1, b_2]$, then it holds that*

$$J(L, K_1) + J(L, K_2) \equiv a_1 + b_1 \equiv a_2 + b_2 \pmod{2}.$$

Proof. By Proposition 5.12, $L = K_1 \cup K_2$ is Ξ -equivalent to a 2-component even virtual link

$$L(c_1, c_2, d_1, d_2; k, l) \text{ or } M(c_1, c_2, d_1, d_2; k, l)$$

for some $c_1, c_2, d_1, d_2, k, l \in \mathbb{Z}$. We only prove the result in the case where L is Ξ -equivalent to $M(c_1, c_2, d_1, d_2; k, l)$. The other case is shown similarly.

By Lemmas 6.5 and 6.9(ii), we have

$$\overline{F}(L) = [c_1, c_2, d_1, d_2 + 1] = [a_1, a_2, b_1, b_2].$$

Therefore it holds that

$$(c_1, c_2, d_1, d_2 + 1) = (a_1, a_2, b_1, b_2) \text{ or } (a_2, a_1, b_2, b_1).$$

In the case $(c_1, c_2, d_1, d_2 + 1) = (a_1, a_2, b_1, b_2)$, since L is Ξ -equivalent to

$$M(c_1, c_2, d_1, d_2; k, l) = M(a_1, a_2, b_1, b_2 - 1; k, l),$$

it holds that

$$J(L, K_1) + J(L, K_2) = (2k + 1) + (a_2 + b_2 - 1 + 2l) \equiv a_2 + b_2 \pmod{2}$$

by Lemma 6.2 and 6.9(ii). Since $M(a_1, a_2, b_1, b_2 - 1; k, l)$ is even, Lemma 6.8(ii) gives

$$a_1 + b_1 \equiv a_2 + b_2 \pmod{2}.$$

Therefore we have

$$J(L, K_1) + J(L, K_2) \equiv a_2 + b_2 \equiv a_1 + b_1 \pmod{2}.$$

In the case $(c_1, c_2, d_1, d_2 + 1) = (a_2, a_1, b_2, b_1)$, L is Ξ -equivalent to

$$M(c_1, c_2, d_1, d_2; k, l) = M(a_2, a_1, b_2, b_1 - 1; k, l).$$

Similarly to the first case, we have

$$\begin{aligned} J(L, K_1) + J(L, K_2) &= (2k + 1) + (a_1 + b_1 - 1 + 2l) \\ &\equiv a_1 + b_1 \equiv a_2 + b_2 \pmod{2}. \end{aligned}$$

\square

The relationship in Theorem 6.10 is considered as a necessary condition for integers to be the reduced linking class of a 2-component even virtual link. It is also a sufficient condition as follows.

Proposition 6.11. *For any integers a_1, a_2, b_1 and b_2 with $a_1 + b_1 \equiv a_2 + b_2 \pmod{2}$, there exists a 2-component even virtual link $L = K_1 \cup K_2$ such that*

- (i) $\overline{F}(L) = [a_1, a_2, b_1, b_2]$ and
- (ii) $J(L, K_1) + J(L, K_2) \equiv a_1 + b_1 \equiv a_2 + b_2 \pmod{2}$.

Proof. Let $L = K_1 \cup K_2$ be the 2-component virtual link $L(a_1, a_2, b_1, b_2; k, l)$ for some $k, l \in \mathbb{Z}$. Then L is even by Lemma 6.8(i). Furthermore, it holds that

$$\overline{F}(L) = [a_1, a_2, b_1, b_2] \text{ and } J(L, K_1) + J(L, K_2) = a_2 + b_2 + 2k + 2l$$

by Lemma 6.9(i). Therefore L satisfies (i) and (ii). \square

We remark that the 2-component even virtual link $M(a_1, a_2, b_1, b_2 - 1; k, l)$ also satisfies (i) and (ii) in Proposition 6.11.

7. PROOF OF THEOREM 1.3

The set of representatives of 2-component virtual links under Ξ -equivalence given in Proposition 5.12 is not complete; that is, there are Ξ -equivalent pairs of virtual links in the sets of $L(a_1, a_2, b_1, b_2; k, l)$'s and $M(a_1, a_2, b_1, b_2; k, l)$'s. For example, it is easily seen using the deformation (2) in Lemma 4.3, that $L(1, 0, 0, 1; 0, 0)$ and $L(0, 1, 1, 0; 0, 0)$ are Ξ -equivalent. Generally we have the following.

Proposition 7.1. *We have the following.*

(i) *If $L(a_1, a_2, b_1, b_2; k, l)$ is even, then it is Ξ -equivalent to*

$$L(a_2, a_1, b_2, b_1; k, l + \frac{1}{2}(-a_1 + a_2 - b_1 + b_2)).$$

(ii) *If $M(a_1, a_2, b_1, b_2; k, l)$ is even, then it is Ξ -equivalent to*

$$M(a_2, a_1, b_2 + 1, b_1 - 1; k, l + \frac{1}{2}(-a_1 + a_2 - b_1 + b_2 + 1)).$$

To prove this proposition, we prepare the following lemma.

Lemma 7.2. *We have the Ξ -equivalence $B_4 \sim B_1 B_2^{-1} B_3$ up to shell-pairs.*

Proof. Since it holds that $B_4 \sim B_1 B_2 B_3^{-1}$ by $B_1 B_2 \sim B_4 B_3$ in Lemma 5.7(i) and $B_3^{-1} \sim B_2^{-2} B_3$ by Lemma 5.8, we have

$$B_4 \sim B_1 B_2 B_3^{-1} \sim B_1 B_2 (B_2^{-2} B_3) \sim B_1 B_2^{-1} B_3.$$

\square

Proof of Proposition 7.1. Since the proofs of (i) and (ii) are similar, we only prove (ii) by giving the Ξ -equivalence of the Gauss diagrams

$$H(a_1, a_2, b_1, b_2; k, l) \sim H(a_2, a_1, b_2 + 1, b_1 - 1; k, l + \frac{1}{2}(-a_1 + a_2 - b_1 + b_2 + 1)).$$

We remark that $a_1 + a_2 + b_1 + b_2$ is odd by Lemma 6.8(ii).

Put $G = H(a_1, a_2, b_1, b_2; k, l)$. Let G_1 be the Gauss diagram obtained from G by adding a free chord γ on C_2 at the top of the ladder of G by an R1-move as shown in Figure 7.1(A). Let P be the terminal endpoint of γ . We will slide P along the vertical line of the ladder of G_1 from top to bottom as follows.

First we exchange the positions of P and $|a_1|$ terminal endpoints of the nonself-chords labeled $A_1^{e(a_1)}$ by using the deformations (1) and (2) in Lemma 4.3 alternately. The deformations are similar to those used in the proof of Proposition 5.12. As a result, the terminal endpoint of each nonself-chord labeled $A_1^{e(a_1)}$ gets a shell so that the label of the chord turns into $A_2^{e(a_1)}$. We remark that P has (resp. does not have) a shell after this deformation if a_1 is odd (resp. even). See Figure 7.1(B), where the potential shell at P depending on the parity of a_1 is indicated by a dashed arc.

Next we exchange the positions of P and $|a_2|$ terminal endpoints of nonself-chords labeled $A_2^{e(a_2)}$ by using the deformations (2) and (3) in Lemma 4.3 alternately. As a result, the terminal endpoint of each nonself-chord labeled $A_2^{e(a_2)}$ loses its shell, so that the label of the chord turns into $A_1^{e(a_2)}$. Furthermore P has (resp. does not have) a shell if $a_1 + a_2$ is odd (resp. even). See Figure 7.1(C).

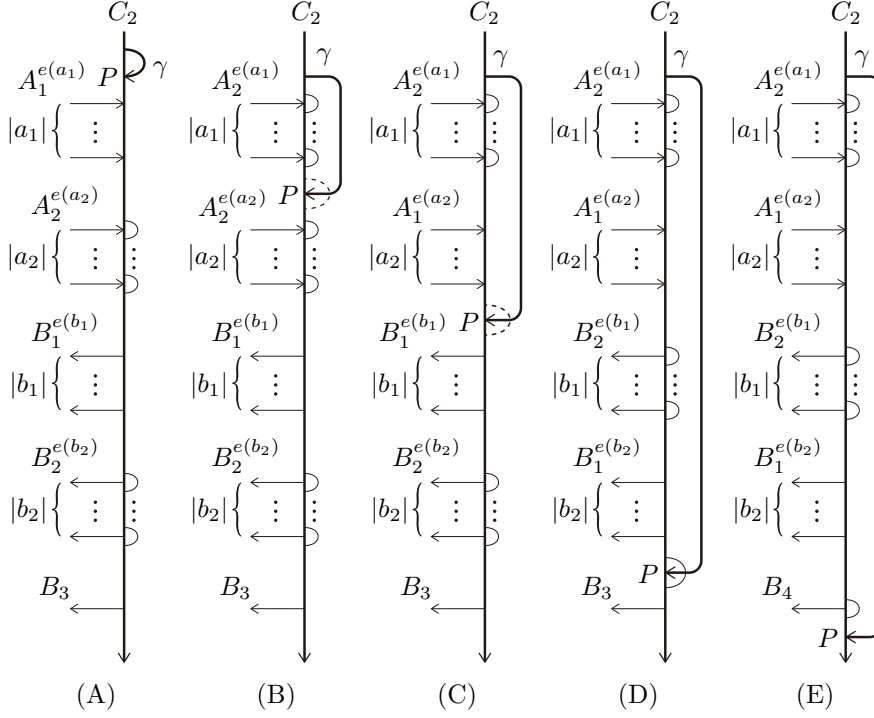


FIGURE 7.1. Proof of Proposition 7.1

Similarly, we exchange the positions of P and $|b_1|$ initial endpoints of the nonself-chords labeled $B_1^{e(b_1)}$, and then the positions of P and $|b_2|$ initial endpoints of the nonself-chords labeled $B_2^{e(b_2)}$. As a result, the label of each nonself-chord labeled $B_1^{e(b_1)}$ (resp. $B_2^{e(b_2)}$) turns into $B_2^{e(b_1)}$ (resp. $B_1^{e(b_2)}$). Since $a_1 + a_2 + b_1 + b_2$ is odd, P has a shell at this point. See Figure 7.1(D).

Finally we exchange the positions of P and the initial endpoint of the nonself-chord labeled B_3 by the deformation (2) in Lemma 4.3 so that the label of the chord turns into B_4 . We remark that P does not have a shell. See Figure 7.1(E).

Since the positions of P and any shell-pair on C_2 can be exchanged by Lemma 4.1, we move P next to the initial endpoint of γ , and then remove γ by an R1-move. Let G_2 be the obtained Gauss diagram with the ladder $A_2^{a_1} A_1^{a_2} B_2^{b_1} B_1^{b_2} B_4$. By Lemma 7.2, followed by Lemmas 5.3, 5.6, and 5.7, we have

$$A_2^{a_1} A_1^{a_2} B_2^{b_1} B_1^{b_2} B_4 \sim A_2^{a_1} A_1^{a_2} B_2^{b_1} B_1^{b_2} (B_1 B_2^{-1} B_3) \sim A_1^{a_2} A_2^{a_1} B_1^{b_2+1} B_2^{b_1-1} B_3$$

up to shell-pairs on C_2 . Therefore G_2 is Ξ -equivalent to

$$G_3 = H(a_2, a_1, b_2 + 1, b_1 - 1; k, l')$$

for some $l' \in \mathbb{Z}$.

By Lemma 6.9(ii), we have

$$J(G, C_2) = a_2 + b_2 + 2l \text{ and } J(G_3, C_2) = a_1 + (b_1 - 1) + 2l'.$$

Since G and G_3 are Ξ -equivalent, it follows by Lemma 6.2 that

$$l' = l + \frac{1}{2}(-a_1 + a_2 - b_1 + b_2 + 1).$$

□

Proof of Theorem 1.3. (i) \Rightarrow (ii). This follows from Lemmas 6.2 and 6.5 directly.

(ii) \Rightarrow (i). By Proposition 5.12, $L = K_1 \cup K_2$ is Ξ -equivalent to either

$$L(a_1, a_2, b_1, b_2; k, l) \text{ or } M(a_1, a_2, b_1, b_2; k, l)$$

for some $a_1, a_2, b_1, b_2, k, l \in \mathbb{Z}$. We only prove the result in the case where L is Ξ -equivalent to $M(a_1, a_2, b_1, b_2; k, l)$. The other case is shown similarly.

Since the odd writhe $J(L, K_1)$ of the pair (L, K_1) is odd by Lemma 6.9(ii), so is $J(L', K'_1)$ by the assumption $J(L, K_1) = J(L', K'_1)$. Therefore L' is Ξ -equivalent to $M(a'_1, a'_2, b'_1, b'_2; k', l')$ for some $a'_1, a'_2, b'_1, b'_2, k', l' \in \mathbb{Z}$ by Proposition 5.12 and Lemma 6.9(ii). Then it holds that

$$2k+1 = 2k'+1, \quad a_2+b_2+2l = a'_2+b'_2+2l', \quad \text{and} \quad [a_1, a_2, b_1, b_2+1] = [a'_1, a'_2, b'_1, b'_2+1]$$

by assumption and Lemma 6.9(ii).

We have $k = k'$ by the first equation above, and

$$(a_1, a_2, b_1, b_2+1) = (a'_1, a'_2, b'_1, b'_2+1) \text{ or } (a'_2, a'_1, b'_2+1, b'_1)$$

by the third equation. In the case $(a_1, a_2, b_1, b_2+1) = (a'_1, a'_2, b'_1, b'_2+1)$, we have $l = l'$ by the second equation to obtain

$$M(a_1, a_2, b_1, b_2; k, l) = M(a'_1, a'_2, b'_1, b'_2; k', l').$$

Therefore L is Ξ -equivalent to L' . In the case $(a_1, a_2, b_1, b_2+1) = (a'_2, a'_1, b'_2+1, b'_1)$, we have $l = l' + \frac{1}{2}(-a'_1 + a'_2 - b'_1 + b'_2 + 1)$ by the second equation to obtain

$$M(a_1, a_2, b_1, b_2; k, l) = M(a'_2, a'_1, b'_2+1, b'_1-1; k', l' + \frac{1}{2}(-a'_1 + a'_2 - b'_1 + b'_2 + 1)).$$

Since this link is Ξ -equivalent to $M(a'_1, a'_2, b'_1, b_2; k', l')$ by Proposition 7.1(ii), L is Ξ -equivalent to L' . \square

We consider the following subsets of 2-component even virtual links;

$$X_1 = \{L(a_1, a_2, b_1, b_2; k, l) \mid a_1 + a_2 + b_1 + b_2 \equiv 0 \pmod{2} \text{ and } a_1 < a_2\},$$

$$X_2 = \{L(a_1, a_1, b_1, b_2; k, l) \mid b_1 + b_2 \equiv 0 \pmod{2} \text{ and } b_1 \leq b_2\},$$

$$Y_1 = \{M(a_1, a_2, b_1, b_2; k, l) \mid a_1 + a_2 + b_1 + b_2 \equiv 1 \pmod{2} \text{ and } a_1 < a_2\}, \text{ and}$$

$$Y_2 = \{M(a_1, a_1, b_1, b_2; k, l) \mid b_1 + b_2 \equiv 1 \pmod{2} \text{ and } b_1 \leq b_2 + 1\}.$$

Corollary 7.3. *The sets X_1, X_2, Y_1 and Y_2 satisfy the following.*

- (i) *The sets X_1, X_2, Y_1 , and Y_2 are mutually disjoint.*
- (ii) *There is no distinct pair of 2-component even virtual links in X_1, X_2, Y_1 , or Y_2 which are Ξ -equivalent.*
- (iii) *The disjoint union $X_1 \sqcup X_2 \sqcup Y_1 \sqcup Y_2$ is a complete representative system of the Ξ -equivalence classes of 2-component even virtual links.*

Proof. The odd writhe $J(L, K_1)$ in Lemma 6.9 induces that $X_1 \cup X_2$ and $Y_1 \cup Y_2$ are disjoint. Furthermore, the reduced linking class $\overline{F}(L)$ in the lemma induces that $X_1 \cap X_2 = \emptyset$ and $Y_1 \cap Y_2 = \emptyset$.

(ii) Assume that two virtual links $L = K_1 \cup K_2 = L(a_1, a_2, b_1, b_2; k, l)$ and $L' = K'_1 \cup K'_2 = L(a'_1, a'_2, b'_1, b'_2; k', l')$ in X_1 are Ξ -equivalent. It follows from $a_1 < a_2, a'_1 < a'_2$, and $\overline{F}(L) = \overline{F}(L')$ that

$$a_1 = a'_1, \quad a_2 = a'_2, \quad b_1 = b'_1, \quad \text{and} \quad b_2 = b'_2.$$

Then we have $k = k'$ and $l = l'$ by $J(L, K_1) = J(L', K'_1)$ and $J(L, K_2) = J(L', K'_2)$. Since L and L' coincide, there is no distinct pair of 2-component even virtual links in X_1 which are Ξ -equivalent.

Assume that two virtual links $L = K_1 \cup K_2 = L(a_1, a_1, b_1, b_2; k, l)$ and $L' = K'_1 \cup K'_2 = L(a'_1, a'_1, b'_1, b'_2; k', l')$ in X_2 are Ξ -equivalent. Since $b_1 \leq b_2, b'_1 \leq b'_2$, and $\overline{F}(L) = \overline{F}(L')$ hold, we have $b_1 = b'_1$ and $b_2 = b'_2$. Then we have $k = k'$ and $l = l'$ by $J(L, K_1) = J(L', K'_1)$ and $J(L, K_2) = J(L', K'_2)$. Therefore there is no distinct

pair of 2-component even virtual links in X_2 which are Ξ -equivalent. Similarly we can prove that this is the case for Y_1 and Y_2 .

(iii) We will prove that any 2-component even virtual link L is Ξ -equivalent to some virtual link belonging to $X_1 \sqcup X_2 \sqcup Y_1 \sqcup Y_2$. By Proposition 5.12, L can be written in the form

$$L(a_1, a_2, b_1, b_2; k, l) \text{ or } M(a_1, a_2, b_1, b_2; k, l)$$

for some $a_1, a_2, b_1, b_2, k, l \in \mathbb{Z}$.

In the case $L = L(a_1, a_2, b_1, b_2; k, l)$, it follows from Lemma 6.8(i) that

$$a_1 + a_2 + b_1 + b_2 \equiv 0 \pmod{2}.$$

By Proposition 7.1(i), we may assume that L satisfies $a_1 \leq a_2$. For $a_1 < a_2$, we have $L \in X_1$. For $a_1 = a_2$, we have $b_1 + b_2 \equiv 0 \pmod{2}$. Furthermore, we may assume that $b_1 \leq b_2$ by Proposition 7.1(i). Then it holds that $L \in X_2$.

In the case $L = M(a_1, a_2, b_1, b_2; k, l)$, we can similarly prove that L is Ξ -equivalent to some virtual link belonging to Y_1 or Y_2 . \square

REFERENCES

- [1] B. Audoux, P. Bellingeri, J.-B. Meilhan, and E. Wagner, *Extensions of some classical local moves on knot diagrams*, Michigan Math. J. **67** (2018), 647–672.
- [2] Z. Cheng and H. Gao, *A polynomial invariant of virtual links*, J. Knot Theory Ramifications **22** (2013), no. 12, 1341002, 33 pp.
- [3] M. Goussarov, M. Polyak, and O. Viro, *Finite-type invariants of classical and virtual knots*, Topology **39** (2000), no. 5, 1045–1068.
- [4] T. Kanenobu, *Forbidden moves unknot a virtual knot*, J. Knot Theory Ramifications **10** (2001), no. 1, 89–96.
- [5] L. H. Kauffman, *Virtual knot theory*, European J. Combin. **20** (1999), no. 7, 663–690.
- [6] L. H. Kauffman, *A self-linking invariant of virtual knots*, Fund. Math. **184** (2004), 135–158.
- [7] H. A. Miyazawa, K. Wada, and A. Yasuhara, *Linking invariants of even virtual links*, J. Knot Theory Ramifications **26** (2017), no. 12, 1750072, 12 pp.
- [8] T. Nakamura, Y. Nakanishi, and S. Satoh, *Writhe polynomials and shell moves for virtual knots and links*, European J. Combin. **84** (2020), 103033, 24 pp.
- [9] T. Nasybullov, *Classification of fused links*, J. Knot Theory Ramifications **25** (2016), no. 14, 1650076, 21 pp.
- [10] S. Nelson, *Unknotting virtual knots with Gauss diagram forbidden moves*, J. Knot Theory Ramifications **10** (2001), no. 6, 931–935.
- [11] Y. Ohyama and M. Yoshikawa, *A writhe of a virtual knot and a local move* (in Japanese), Proceedings of Mathematics of Knots V (2013), 89–96. Available at <http://www.f.waseda.jp/taniyama/math-of-knots-v/report/all.pdf>
- [12] T. Okabayashi, *Forbidden moves for virtual links*, Kobe J. Math. **22** (2005), no. 1–2, 49–63.
- [13] S. Satoh and K. Taniguchi, *The writhes of a virtual knot*, Fund. Math. **225** (2014), no. 1, 327–341.

UNIV. GRENOBLE ALPES, CNRS, IF, 38000 GRENOBLE, FRANCE
Email address: jean-baptiste.meilhan@univ-grenoble-alpes.fr

DEPARTMENT OF MATHEMATICS, KOBE UNIVERSITY, ROKKODAI-CHO 1-1, NADA-KU, KOBE 657-8501, JAPAN
Email address: shin@math.kobe-u.ac.jp

DEPARTMENT OF MATHEMATICS, KOBE UNIVERSITY, ROKKODAI-CHO 1-1, NADA-KU, KOBE 657-8501, JAPAN
Email address: wada@math.kobe-u.ac.jp